2. *trans*-Co(CN)₃(H₂O)₃.[7] Although the detailed examples in the previous sections were all concerned with d³ systems, an extension to d⁶ systems is quite straightforward.[11] The adequate coordinate system is shown in Figure 4. The ligand field parameters were taken from a detailed spectroscopic analysis of a number of mixed aquo–cyano–cobalt(III) complexes[12] (all values in μm^{-1}): σ_{CN^-}, 1.215; σ_{H_2O}, 0.66; C, 0.360; π_{CN^-}, 0.039; π_{H_2O}, 0.108; B, 0.053; $10Dq_{CN^-}$, 3.489; $10Dq_{H_2O}$, 1.547. In this complex, $\bar{\sigma}_y = {}^1/_2(\bar{\sigma}_z + \bar{\sigma}_x)$, which implies that $\tan 2\alpha = 1/3^{1/2}$ and $\alpha = 105°$. Calculating the combined effect of the orthorhombic field and the interelectronic repulsion, one obtains $\theta = 100.83°$ and $1a_g \simeq 0.982(x^2 - y^2) - 0.188(z^2)$.

The lowest excited $^3B_{1g}$ state ($xy \rightarrow 1a_g$) is characterized by

$$I^* = \epsilon(xy) + (1a_g|V|1a_g) + 2(2a_g|V|2a_g)$$

$$I^*(ML_z) = 1.96\sigma_z \quad I^*(Co-(CN)_z) = 2.39 \ \mu m^{-1}$$

$$I^*(ML_y) = 1.43\sigma_y + \pi_y \quad I^*(Co-(CN)_y) = 1.77 \ \mu m^{-1}$$
$$I^*(Co-(H_2O)_y) = 1.05 \ \mu m^{-1}$$

$$I^*(ML_x) = 1.11\sigma_x + \pi_x \quad I^*(Co-(H_2O)_x) = 0.84 \ \mu m^{-1}$$

Therefore, one expects the solvent ligands on the x axis to be preferentially exchanged upon ligand field irradiation. This is again compatible with an application of Adamson's rules to the D_{2h} case. The experimentally observed photoinertness of *trans*-Co(CN)₃(H₂O)₃ in aqueous solution is compatible with the predictions, but so far the possibility of (H₂O)$_y$ labilization cannot be excluded.

3. *cis*-Rh(NH₃)₄(H₂O)Cl²⁺,[8] *cis*-Rh(NH₃)₄(H₂O)Br²⁺,[8] and *cis*-Rh(en)₂(H₂O)Br²⁺.[9] For the Rh(III) parameters, the following numbers have been derived from a spectral analysis[12] (all values in μm^{-1}): σ_{NH_3}, 1.14; σ_{Cl^-}, 0.88; σ_{Br^-}, ~0.93; π_{NH_3}, 0; π_{Cl^-}, 0.21; π_{Br^-}, 0.29; B, ~0.04.

The water parameters are less well-known, except for the fact that $10Dq \approx 2.2 \ \mu m^{-1}$. We will assume $\pi_{H_2O} \simeq 0.05$ and $\sigma_{H_2O} = 0.8 \ \mu m^{-1}$. Adopting the coordinate system of Figure 4, one can readily obtain the relevant quantities $\alpha = 96.5$ and 102° and $\theta \simeq 96.2$ and 100.7° for Cl⁻ and Br⁻, respectively. The $1a_g$ orbitals are given by $1a_g(Cl^-) \simeq 0.994(x^2 - y^2) - 0.107(z^2)$ and $1a_g(Br^-) \simeq 0.983(x^2 - y^2) - 0.186(z^2)$, and for the $^3B_{1g}$ state ($xy \rightarrow 1a_g$) in the chloro complex one finds

$$I^*(ML_x) = 1.988\sigma_z \quad I^*(Rh-(NH_3)_z) = 2.27 \ \mu m^{-1}$$

$$I^*(ML_y) = \pi_y + 1.347\sigma_y \quad I^*(Rh-(NH_3)_y) = 1.54 \ \mu m^{-1}$$
$$I^*(Rh-Cl^-) = 1.40 \ \mu m^{-1}$$

$$I^*(ML_x) = \pi_x + 1.163\sigma_x \quad I^*(Rh-(NH_3)_x) = 1.33 \ \mu m^{-1}$$
$$I^*(Rh-H_2O) = 0.98 \ \mu m^{-1}$$

In the bromo complex, one obtains nearly the same bond indices[13] for NH₃ and H₂O, while $I^*(Rh-Br^-) = 1.54 \ \mu m^{-1}$. Clearly, the photoactive $^3B_{1g}$ state will most readily release its H₂O ligand—the uncertainty on the H₂O parameters is definitely smaller than the differences between the I^* values.[14] This conclusion is in agreement with the observation that ligand field excitation of *cis*-Rh(NH₃)₄(H₂O)X²⁺ leads to *trans*-Rh(NH₃)₄(H₂O)X²⁺. These results have been interpreted[8] in terms of a dissociative reaction mechanism, where the isomerization of the pentacoordinated intermediate Rh-(NH₃)₄X²⁺ is held responsible for the observed stereomobility. It should also be stressed that an extension of Adamson's rules leads to the wrong predictions: the strongest ligand on the weakest axis is (NH₃)$_y$.

Conclusions

The bond index formalism is a versatile tool in the comparative study of the different metal–ligand bond strengths within any one given electronic state.

It is possible to adapt this formalism to D_{2h} molecules; the results are sometimes, but not always, similar to Adamson's rules. When the conclusions are divergent, the bond index formalism appears to lead to the correct answers. The reason for deviations from Adamson's rules are twofold:

(i) As shown earlier, Adamson's rules are equivalent to postulating that the leaving ligand is the one that absorbs the most energy and is therefore characterized by the maximal value of $\Delta I(ML) = I(ML) - I^*(ML)$. In fact, the relevant quantity appears to be $I^*(ML)$, not $\Delta I(ML)$.

(ii) In some cases, the role of the *other* ligands may be important in determining $I(ML)$; the relative position and ligand field parameters of the "inert" ligands determine the numerical value of α and θ to a significant extent.

(11) Such an extension is carried out in detail for D_{4h} in ref 4. It is also shown there how the I^* model can accommodate π-acceptor ligands.

(12) L. G. Vanquickenborne, A. Ceulemans, and D. Beyens, to be submitted for publication.

(13) More specifically, one obtains $I^*(Rh-(NH_3)_z) = 2.24 \ \mu m^{-1}$, $I^*(Rh-(NH_3)_y) = 1.54 \ \mu m^{-1}$, $I^*(Rh-(NH_3)_x) = 1.33 \ \mu m^{-1}$, and $I^*(Rh-H_2O) = 0.98 \ \mu m^{-1}$.

(14) Even with $\pi_{H_2O} = 0.1 \ \mu m^{-1}$, one still obtains $I^*(Rh-Cl) - I^*(Rh-H_2O) > 0.1 \ \mu m^{-1}$.

Contribution from the Department of Chemistry, North Carolina State University, Raleigh, North Carolina 27650

Electronic Structures of [PtL₄·PtL₄X₂]⁴⁺ and NbX₄ Chains

MYUNG-HWAN WHANGBO* and MARY J. FOSHEE

The band structures of the singly bridged [Pt(NH₃)₄·Pt(NH₃)₄X₂]⁴⁺ chain (X = Cl, Br) and the doubly bridged NbX₄ chain (X = Cl, I) were obtained by employing the tight-binding scheme based upon the extended Hückel method. The band gaps and the stabilities of these chains were examined as a function of distortion in their unit cell geometries. In contrast to the case of the singly bridged [Pt(NH₃)₄·Pt(NH₃)₄X₂]⁴⁺ chain, the doubly bridged NbX₄ chain leads to partially filled overlapping bands even if the metal-bridging halide bonds are not exactly the same in length.

Metal–ligand–metal bridging is an important structural pattern leading to numerous chain and net compounds of transition-metal ions.[1-3] In connection with recent interest in low-dimensional conducting materials, a number of lig-

Table I

A. Atomic Parameters[a,b]

μ	ζ_μ	ζ_ν	$H_{\mu\nu}$, eV
Pt 6s	2.554[c]		−9.08
Pt 6p	2.554		−5.48
Pt 5d	6.013 (0.6334)	2.696 (0.5513)	−12.6
Nb 5s	1.90[d]		−10.1
Nb 5p	1.85		−6.86
Nb 4d	4.080 (0.6401)	1.640 (0.5516)	−12.1
I 5s	2.679[e]		−18.0[f]
I 5p	2.322		−12.7
Br 4s	2.640[e]		−22.1[f]
Br 4p	2.260		−13.1
Cl 3s	2.356[e]		−24.2[f]
Cl 3p	2.039		−15.0
N 2s	1.95		−26.0
N 2p	1.95		−13.4
H 1s	1.3		−13.6

B. Geometrical Parameters

(1) **1**, **2**, and **3** (NH_3 molecules arranged such that the chain has the C_{4v} site symmetry): Pt–N = 1.97 Å, N–H = 3.13 Å, ∠HNH = 107°; Pt^{IV}–Cl = 2.26 Å, Pt^{II}–Cl = 3.13 Å; Pt^{IV}–Br = 2.463 Å, Pt^{II}–Br = 3.123 Å

(2) **6** and **7**: for NbCl$_4$ (**6**), Nb–Nb = 3.029, 3.794 Å, Nb–Cl(bridging) = 2.425, 2.523 Å, Nb–Cl(terminal) = 2.291 Å, for NbCl$_4$ (**7**), Nb–Nb = 3.413 Å, Nb–Cl(bridging and terminal) = 2.414 Å; for NbI$_4$ (**6**), Nb–Nb = 2.89, 3.31 Å, Nb–I(bridging) = 2.74, 2.895 Å, Nb–I(terminal) = 2.675 Å

[a] The d orbitals are given as a linear combination of two Slater type functions, and each is followed in parentheses by the weighting coefficient. [b] A modified Wolfsberg–Helmholz formula was used to calculate $H_{\mu\nu}$.[14] [c] Reference 8a. [d] Reference 8b. [e] Reference 15. [f] Reference 16.

and-bridged chain compounds have been the subject of many experimental and theoretical studies.[2,3] Qualitatively the electronic properties of such compounds are described by focusing upon the d orbitals of a single metal ion, but, because of the extended nature of those compounds, a more satisfactory description takes their band electronic structures into consideration. In the present work we are concerned with the band structures of two representative halide-bridged chain compounds, the singly bridged [PtL$_4$·PtL$_4$X$_2$]$^{4+}$ chain[4] and the doubly bridged NbX$_4$ chain.[5] These two chains share a common structural pattern; namely, each chain has two metal-bridging halide bonds of unequal lengths alternating along the chain direction. This structural feature is responsible for the insulating (or semiconducting) property of these chains, but the electrical conductivities of these chains were found to increase sharply with temperature or pressure.[6,7] In ac-

(1) Wells, A. F. "Structural Inorganic Chemistry", 4th ed.; Clarendon: London, 1975.
(2) (a) Miller, J. S.; Epstein, A. J. *Prog. Inorg. Chem.* **1976**, *20*, 1. (b) Stucky, G.; Schultz, A. J.; Williams, J. M. *Annu. Rev. Mater. Sci.* **1977**, *7*, 301.
(3) (a) Keller, H. J., Ed. "Low-Dimensional Cooperative Phenomena"; Plenum: New York, 1974. (b) Keller, H. J., Ed. "Chemistry and Physics of One-Dimensional Metals"; Plenum: New York, 1977. (c) Miller, J. S.; Epstein, A. J., Eds. *Ann. N.Y. Acad. Sci.* **1978**, *313*.
(4) (a) Craven, B. M.; Hall D. *Acta Crystallogr.* **1961**, *14*, 475. (b) Bekaroglu, O.; Beer, H.; Endres, H.; Keller, H. J.; Nam Gung, H. *Inorg. Chim. Acta* **1977**, *21*, 183. (c) Brown, K. L.; Hall, D. *Acta Crystallogr.* **1976**, *B32*, 279. (d) Day, P. Reference 3a, p 191; ref 3b, 197. (e) Clark, R. J. H.; Franks, M. L.; Trumble, W. R. *Chem. Phys. Lett.* **1976**, *41*, 287. (f) Mayoh, B.; Day, P. *J. Chem. Soc., Dalton Trans.* **1973**, 846. (g) Clark, R. J. H. Reference 3c, p 672. (h) Endres, H.; Sharif, M. E.; Keller, H. J.; Martin, R.; Trager, J. Reference 3c, p 663. (i) Robin, M. B.; Day, P. *Adv. Inorg. Radiochem.* **1967**, *10*, 247.
(5) (a) Taylor, D. R.; Calabrese, J. C.; Larsen, E. M. *Inorg. Chem.* **1977**, *16*, 721. (b) Dahl, L. F.; Wampler, D. L. *Acta Crystallogr.* **1962**, *15*, 903. (c) Blight, D. G.; Kerpert, D. L. *Phys. Rev. Lett.* **1971**, *27*, 504. (d) Schafer, H.; Dohmann, D.-D. *Z. Anorg. Allg. Chem.* **1961**, *311*, 134. (e) Seabaugh, P. W.; Corbett, J. D. *Inorg. Chem.* **1965**, *4*, 176.

Figure 1. Calculated d-block band orbital energies of the [Pt-(NH$_3$)$_4$·Pt(NH$_3$)$_4$Cl$_2$]$^{4+}$ chain **2** as a function of wave vector, k.

counting for such a change in the electrical properties, it is important to examine how the stability and the band gap of an extended linear chain are affected by geometry distortion of its repeat unit,[2b,7] since the electrical properties follow the structural and ultimately the electronic properties. In the following this structure–property relationship is explored for the [PtL$_4$·PtL$_4$X$_2$]$^{4+}$ and NbX$_4$ chains by studying their one-electron band structures determined from the tight-binding scheme[8] based upon the extended Hückel method.[9] This methodology of band structure calculation was described in some detail elsewhere[8a] and was found quite satisfactory in describing a wide range of organic and inorganic structural problems.[8] The atomic and geometrical parameters employed in our calculations are summarized in Table I.

Results and Discussion

A. [Pt^{II}L$_4$·Pt^{IV}L$_4$X$_2$]$^{4+}$ Chain. Wolffram's red salt and its analogues[4,7] have singly bridged linear arrays of alternating Pt^{II}L$_4$ and Pt^{IV}L$_4$X$_2$ complex units as schematically shown in **1**. It is convenient to consider **1** as a distorted structure of
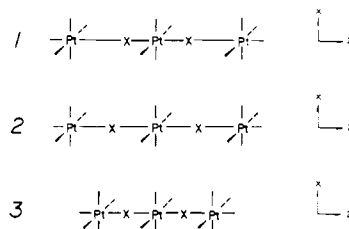
an ideal chain of Pt^{III}L$_4$X units such as **2** or **3**. The chain **2** has the bridging halide ions located at the midpoints between the metal ions of **1**, while the chain **3** is obtained from **1** by reducing the Pt^{II}–X bond to the value of the Pt^{IV}–X bond length. The energy barriers of the distortions **1** → **2** and **1**

(6) (a) Kerpert, D. L.; Marshall, R. E. *J. Less-Common Met.* **1974**, *34*, 153. (b) Kawamura, H.; Shiratani, I.; Tachikawa, K. *Phys. Lett. A* **1978**, *65A*, 335.
(7) (a) Interrante, L. V. Reference 2a, p 299. (b) Interrante, L. V.; Bundy, F. P.; Browall, K. W. *Inorg. Chem.* **1974**, *13*, 1158. (c) Interrante, L. V.; Browall, K. W. *Ibid.* **1974**, *13*, 1162.
(8) (a) Whangbo, M.-H.; Hoffmann, R. *J. Am. Chem. Soc.* **1978**, *100*, 6093. (b) Whangbo, M.-H.; Hoffmann, R.; Woodward, R. B. *Proc. R. Soc. London, Ser. A* **1979**, *366*, 23. (c) Whangbo, M.-H.; Foshee, M. J.; Hoffmann, R. *Inorg. Chem.* **1980**, *19*, 1723.
(9) (a) Hoffmann, R. *J. Chem. Phys.* **1963**, *39*, 1397. (b) Hoffmann, R.; Lipscomb, W. N. *Ibid.* **1962**, *36*, 2179, 3489; **1962**, *37*, 2872.
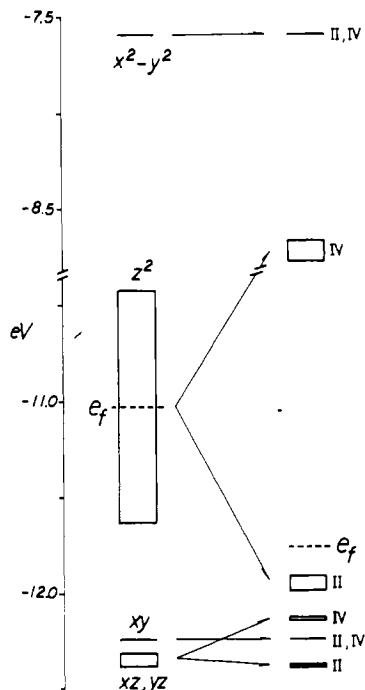
Figure 2. d-Block bands of the $[Pt(NH_3)_4 \cdot Pt(NH_3)_4Cl_2]^{4+}$ chains **1** (right) and **2** (left).

→ **3** may be estimated from the band structures of a $[Pt^{II}-(NH_3)_4 \cdot Pt^{IV}(NH_3)_4Cl_2]^{4+}$ chain, which we chose as a model for the $[Pt^{II}(EtNH_2)_4 \cdot Pt^{IV}(EtNH_2)_4Cl_2]^{4+}$ chain present in Wolffram's red salt.[4a] In the following the structures **1–3** refer to this model chain unless stated otherwise.

Figure 1 shows the d-block bands of **2**, in which the lowest lying band is doubly degenerate. Interactions between the $[Pt^{III}(NH_3)_4Cl]^{2+}$ units occur primarily through the metal–halide–metal bridge along the chain, and hence only the d_{z^2} band has appreciable bandwidth. The nodal properties of the d_{z^2} band orbitals at the zone center ($k = 0$) and edge ($k = \pi/a$, where a is the repeat distance) are depicted in **4a** and **4b**, respectively. The metal d orbitals of neighboring unit cells
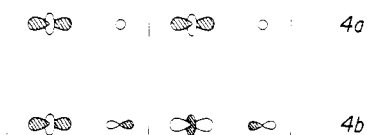
have the same signs at the zone center but the opposite signs at the zone edge. The d orbitals arranged as such combine out of phase with the ligand orbitals of proper symmetry. Since the overlap between the metal and halide ions is more effective with the halogen p_z orbital, **4a** lies lower in energy than **4b**. In agreement with the usual picture of metal–ligand bonding, the metal d orbitals are found to make bonding combinations with the ligand s and p orbitals in the bands of largely ligand characters which lie below the d-block bands.

The unit cell of **2**, $[Pt^{III}(NH_3)_4Cl]^{2+}$, has a d^7 ion, and thus the d_{z^2} band of Figure 1 becomes half-filled. The width of the d_{z^2} band is rather narrow (~ 1.2 eV). Thus, consideration of electron–electron repulsion[2a,10] might suggest a magnetic insulating state for **2**, but the presence of the $Pt^{IV}-X-Pt^{II}$ bond alternation and the pressure-induced increase[7] in the electrical conductivities of Wolffram's red salt and its analogues suggest a nonmagnetic metallic state for **2**.[4d,11]
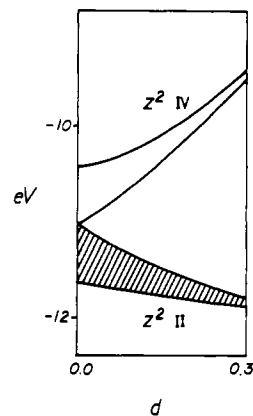
Figure 3. The widths of the $d_{z^2}^{II}$ and $d_{z^2}^{IV}$ bands in the $[Pt-(NH_3)_4 \cdot Pt(NH_3)_4Cl_2]^{4+}$ chain as a function of d (in Å). The shaded area indicates that each band orbital is doubly occupied.
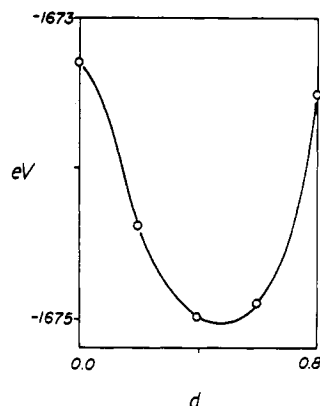
Figure 4. Total energy per $[Pt(NH_3)_4 \cdot Pt(NH_3)_4Cl_2]^{4+}$ unit as a function of d (in Å).

The unit cell of **1**, $[Pt^{II}(NH_3)_4 \cdot Pt^{IV}(NH_3)_4Cl_2]^{4+}$, is twice as large as that of **2**. The energy bands of **1** and **2** shown in Figure 2 reveal that the d_{z^2} band undergoes the most significant change during the distortion **2** → **1**. The $d_{x^2-y^2}$ and d_{xy} orbitals of a metal ion do not overlap with the s and p orbitals of a bridging halide ion, so the $d_{x^2-y^2}$ and d_{xy} bands are not affected by the distortion but become practically degenerate in **1** because of the doubled unit cell size. Of the two split bands resulting from the d_{z^2} or the $d_{xz,yz}$ band, the lower (upper) one is made up of largely the d orbitals of the $Pt^{II}(Pt^{IV})$ ions with small contribution from the d orbitals of the $Pt^{IV}(Pt^{II})$ ions. At the zone center, the magnitudes of the d_{z^2} orbital coefficients of the Pt^{II} and Pt^{IV} ions are respectively 0.92 and 0.15 in the $d_{z^2}^{II}$ band orbital, while they are respectively 0.12 and 0.91 in the $d_{z^2}^{IV}$ band orbital. This delocalization between the Pt^{II} and Pt^{IV} ions, which occurs through the bridging halide ions, is responsible for the intense metal-to-metal charge-transfer transition in Wolffram's red salt and its analogues.[4d] With a d^6 and a d^8 ion in each unit cell, the d-block bands of **1** are filled up to the $d_{z^2}^{II}$ band leading to a band gap of ~ 3 eV.

As indicated in **5**, various structures between **2** and **1** can
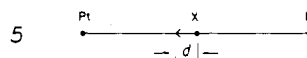
be defined by the distance d from the midpoint between the metal ions to the bridging halogen. Plotted in Figure 3 are

(10) (a) Brandow, B. H. *Adv. Phys.* **1977**, *26*, 651; *Int. J. Quantum Chem., Symp.* **1976**, *10*, 417 and references therein. (b) Whangbo, M.-H. *J. Chem. Phys.* **1979**, *70*, 4963. (c) Whangbo, M.-H. *Inorg. Chem.* **1980**, *19*, 1728.

(11) (a) Ionov, S. P.; Ionova, G. V.; Makarov, E. F.; Aleksandrov, A. T. *Phys. Status Solidi B* **1974**, *64*, 79. (b) Ionov, S. P.; Ionova, G. V.; Lubinov, V. S.; Makarov, E. F. *Ibid.* **1975**, *71*, 11. (c) Whangbo, M.-H. *J. Chem. Phys.* **1980**, *73*, 3854.
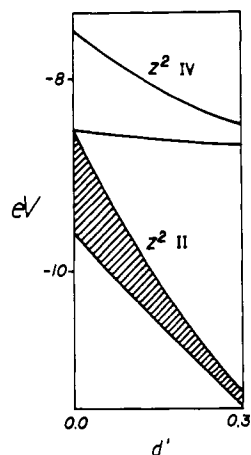
Figure 5. Widths of the $d_{z^2}^{II}$ and $d_{z^2}^{IV}$ bands in the [Pt(NH$_3$)$_4$·Pt-(NH$_3$)$_4$Cl$_2$]$^{4+}$ chain as a function of the Pt^{II}-Pt^{IV} distance, where d' (in Å) = r(Pt^{II}-X) - r(Pt^{IV}-X). The shaded area indicates that each band orbital is doubly occupied.
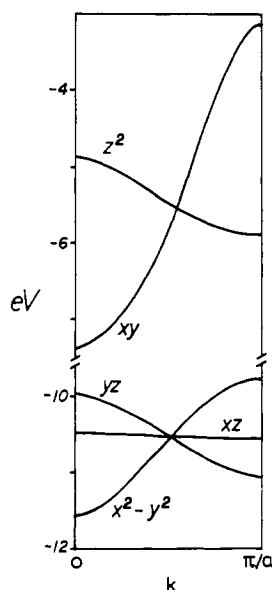
Figure 6. d-Block band orbital energies of the NbCl$_4$ chain **7** as a function of wave vector, k.

the widths of the $d_{z^2}^{II}$ and $d_{z^2}^{IV}$ bands as a function of d. The band gap vanishes at $d = 0$ and increases gradually with d. The total energies per [Pt^{II}(NH$_3$)$_4$·Pt^{IV}(NH$_3$)$_4$Cl$_2$]$^{4+}$ unit, calculated from the band structures[8] were summarized in Figure 4. The energy minimum is found to occur at $d \simeq 0.48$ Å, in good agreement with the experimental value of 0.435 Å in Wolffram's red salt,[4a] and the distortion **1 → 2** is estimated to require ~40 kcal/mol per [Pt^{II}(NH$_3$)$_4$·Pt^{IV}-(NH$_3$)$_4$Cl$_2$]$^{4+}$ unit.

A sharp increase with pressure in the electrical conductivities of Wolffram's red salt and its analogues[7] is believed to arise from a pressure-induced distortion such as **1 → 3**, which reduces the magnitude of the Pt^{IV}-X-Pt^{II} bond alternation along the chain, hence decreasing the band gap.[7] Shown in Figure 5 are the widths of the $d_{z^2}^{II}$ and $d_{z^2}^{IV}$ bands as a function of the Pt^{II}-Pt^{IV} distance. It is expected from **4a** and **4b** that the distortion **1 → 3** would increase the antibonding interaction between the metal and halide ions. Thus the $d_{z^2}^{II}$ and $d_{z^2}^{IV}$ bands are destabilized as **1 → 3**, and the d_{z^2} band of **3** becomes broader than that of **2**. In terms of the calculated total energies per unit cell, the energy barrier of the distortion **1 → 3** is about twice that of the distortion **1 → 2**. Hence the actual geometry change in **1** under high pressure might involve some length-

ening of the Pt^{IV}-X bond in addition to the Pt^{II}-X bond shortening.

Band structures were also calculated for a [Pt^{II}(NH$_3$)$_4$·Pt^{IV}(NH$_3$)$_4$Br$_2$]$^{4+}$ chain, which is chosen as a model for the [Pt^{II}(EtNH$_2$)$_4$·Pt^{IV}(EtNH$_2$)$_4$Br$_2$]$^{4+}$ chain present in Reihlen's green salt.[4c] Compared with the chloride-bridged chain discussed above, the band gap of **1** is slightly decreased in the bromide analogue (~2.8 eV). The calculated barriers of the distortions **1 → 2** and **1 → 3** are significantly smaller in the bromide-bridged chain (i.e., ~23 and ~38 kcal/mol per [Pt(NH$_3$)$_4$·Pt^{IV}(NH$_3$)$_4$Br$_2$]$^{4+}$ unit, respectively, which are approximately half the corresponding values in the chlorine analogue). This result may be due in part to the fact that the bromide-bridged chain involves less geometrical distortion[4g] (e.g., the distortion **1 → 2** moves the bridging halide ion by 0.44 and 0.33 Å in the chloride- and bromide-bridged chains, respectively). It is noted[4g] that the harmonic frequency of the symmetric X-Pt^{IV}-X stretch is greater in Wolffram's red salt than in Reihlen's green salt by a factor of roughly 2.

B. NbX$_4$ Chain. As illustrated in **6**, NbX$_4$ chain consists
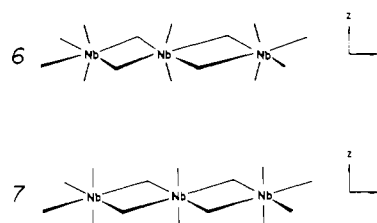
of the structure derived from sharing opposite edges of NbX$_6$ octahedra. **6** has the Nb-X-Nb bonds alternating along the chain and may be regarded as distorted from the ideal edge-sharing octahedral chain **7**, whose Nb-Nb distance is half the repeat distance of **6**. With NbCl$_4$ as an example, the energy barrier of the distortion **6 → 7** and the associated band gap change may now be examined.

The d-block bands of **7** shown in Figure 6 exhibit three-below-two overlapping bands, reflecting the locally octahedral environment of a metal ion. The d_{xz} orbitals of metal ions are pointed away from the bridging ligands, and the direct overlap between them is small. Thus the d_{xz} band is almost flat. The nodal properties of the $d_{x^2-y^2}$ (d_{yz}) band orbitals at the zone center and edge are shown in **8a** and **8b** (**9a** and **9b**), re-

spectively, where the terminal halide ion orbitals of proper symmetry combine out of phase with the d orbitals but are not shown for simplicity. Inspection of the antibonding interactions between the metal and bridging halide ions makes it clear that **8a** and **9b** are lower in energy than **8b** and **9a**, respectively. The nature of the remaining d-block bands can be similarly described. Since a NbCl$_4$ unit contains a d^1 ion, the $d_{x^2-y^2}$ and d_{yz} bands of **7** become partially filled.
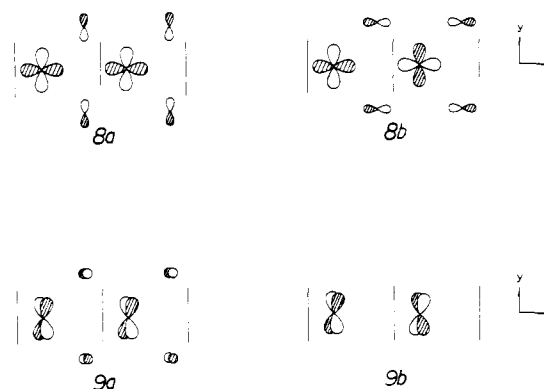
In going to **6** the bottom three d-block bands of **7** split as depicted in Figure 7, where the superscript + (−) of each band means that the major orbital component of that band is the
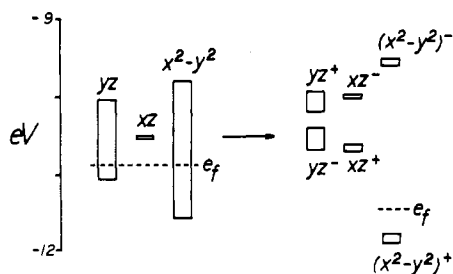
Figure 7. d-Block bands of the NbCl4 chains 6 (right) and 7 (left).
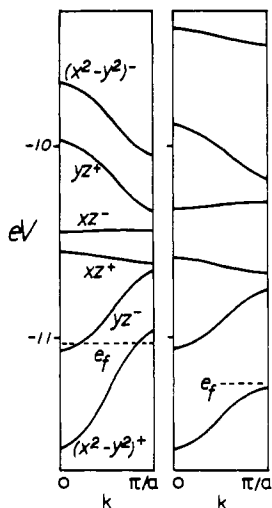
Figure 8. d-Block band orbital energies of the NbCl4 chain as a function of wave vector, k, at $d = 0.1$ (left) and 0.2 Å (right), respectively.

bonding (antibonding) combination of the two d orbitals in a "metal dimer" repeat unit $(NbCl_4)_2$. The metal–metal bonding combination makes an antibonding interaction with the bridging halogen orbitals, and hence the spatial orientation of d orbitals and the metal–metal distance determine whether or not the metal–metal bonding combination lies lower in energy than the corresponding metal–metal antibonding combination.[8c,12] The d-block bands of 6 are now filled up to the $d_{x^2-y^2}{}^+$ band. It is observed that the $d_{x^2-y^2}$ band of 7 corresponds to the d_σ band of NbX4 discussed by Stucky, Schultz, and Williams,[2b] and the d_{xz} and d_{yz} bands of 7 correspond to their d_π band.

A gradual change in structure from 7 to 6 may be approximated by the pairing of metal ions along the chain axis of 7 with positions of other atoms fixed as indicated in 10,
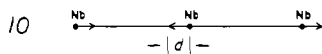
where the distance d measures the magnitude of this distortion. The change in the bottom three d-block bands of 7 is shown in Figure 8 as a function of d. It is noted that the overlap between the $d_{x^2-y^2}{}^+$ and $d_{yz}{}^-$ bands and, thus, their partially filled nature would persist until d reaches a certain value. From the plot of the $d_{x^2-y^2}{}^+$ and $d_{yz}{}^-$ bandwidths vs. d shown in Figure 9, the NbCl4 chain is anticipated to be metallic if $d < \sim 0.12$ Å.

The total energies per $(NbCl_4)_2$ unit calculated as a function of d were summarized in Figure 10. The energy minimum shows up at $d \simeq 0.36$ Å, in good agreement with the exper-

(12) For an analysis of the factor governing metal–metal interactions in dimers and oligomers, see: (a) Summerville, R. H.; Hoffmann, R. *J. Am. Chem. Soc.* **1976**, *98*, 7240; **1979**, *101*, 3821. (b) Shaik, S.; Hoffmann, R.; Fisel, C. R.; Summerville, R. H. *Ibid.* **1980**, *102*, 4555.
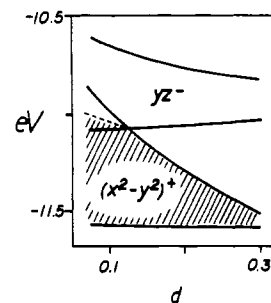
Figure 9. Widths of the $d_{x^2-y^2}{}^+$ and $d_{yz}{}^-$ bands in the NbCl4 chain as a function of d (in Å).
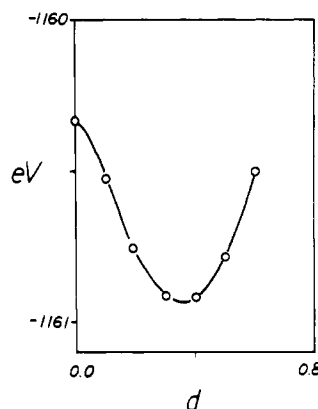
Figure 10. Total energy per $(NbCl_4)_2$ unit as a function of d (in Å).
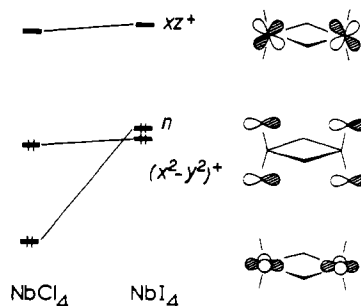
Figure 11. Nodal properties, at the zone center, of band orbitals in the NbCl4 and NbI4 chains.

imental value of 0.383 Å in the NbCl4 chain.[5a] From Figure 10 the energy barrier of the distortion **6 → 7** is estimated to be ~ 14 kcal/mol per $(NbCl_4)_2$ unit. This barrier would be greater than the energy needed for insulator-to-metal transition in 6 since, as already noted, the lengths of the metal-bridging halide bonds need not to be the same for the creation of partially filled bands. This observation is different from the case of the singly bridged chain considered in the previous section. In terms of the pairing distortion 10, the insulator-to-metal transition in 6 is found to require ~ 9 kcal/mol per $(NbCl_4)_2$ unit.

The electrical conductivity of NbX4 increases rapidly with temperature, but NbX4 undergoes disproportionation reactions at high temperature.[2b,6a] Recently it was observed that NbI4 becomes a metal under high pressure.[6b] In view of our results discussed above, the insulator-to-metal transition in NbI4 may be interpreted to be an intrachain phenomenon arising from a pressure-induced reduction in the Nb–X–Nb bond alteration along the chain.

The activation energy for electrical conduction in NbX4 decreases as NbCl4 > NbBr4 > NbI4 despite the increase in the metal–metal distance in the order NbCl4 < NbBr4 < NbI4. This trend has been accounted for by a broadening of the valence (highest occupied) band that originates from an en-

hanced mixing between the ligand p and metal d orbitals with increasing polarizability of X.[6a] The band structures of NbI$_4$ calculated in the present work are consistent with this view. The width of the valence band and the band gap are respectively ~0.3 and ~0.8 eV in NbI$_4$, while the corresponding values are respectively ~0.1 and ~1.0 eV in NbCl$_4$. Figure 11 shows that the lone-pair orbital n of the terminal ligands lies far below the d-block orbital in NbCl$_4$ but slightly above the d$_{x^2-y^2}$+ orbital in NbI$_4$. The proximity of the n and d$_{x^2-y^2}$+ levels in NbI$_4$ causes the valence band to have mixed-orbital characters, largely n near the zone center but d$_{x^2-y^2}$+ near the zone edge.

Concluding Remarks

The halide-bridged [PtL$_4$·PtL$_4$X$_2$]$^{4+}$ and NbX$_4$ chains share a common structural feature; i.e., each chain has two metal-bridging halide bonds of unequal lengths alternating along the chain direction. We found this structural feature well reproduced by the total energies per unit cell calculated from their one-electron band structures. The singly bridged [PtL$_4$·PtL$_4$X$_2$]$^{4+}$ chain provides a partially filled band when all the metal-bridging halide bonds become identical in length while the doubly bridged NbX$_4$ chain, like the triply bridged

VS$_3$$^{2-}$ chain reported elsewhere,[8c] leads to partially filled overlapping bands even if the lengths of the two alternating metal-bridging halide bonds are not exactly the same. However it is noted that a Peierls distortion[2,3] such as the pairing **7** → **6** of the doubly bridged NbX$_4$ chain does not occur in BaVS$_3$ which consists of the triply bridged VS$_3$$^{2-}$ chains.[13]

(13) (a) Takano, M.; Kosugi, H.; Nakamura, N.; Shimada, M.; Wada, T.; Koizumi, M. *J. Phys. Soc. Jpn.* **1977**, 43, 1101. (b) Massenet, O.; Ruder, R.; Since, J. J.; Schlenker, C.; Mercier, J.; Kelber, J.; Stucky, G. D. *Mater. Res. Bull.* **1978**, 13, 187.
(14) Ammeter, J. H.; Bürgi, H.-B.; Thibeault, J. C.; Hoffmann, R. *J. Am. Chem. Soc.* **1978**, 100, 3686.
(15) Clementi, E.; Roetti, C. "Atomic and Nuclear Data Tables"; Academic Press: New York, 1974; Vol. 14, p 177.
(16) Hinze, J.; Jaffe, H. H. *J. Phys. Chem.* **1963**, 67, 1501.

Contribution from the Research Laboratories,
Eastman Kodak Company, Rochester, New York 14650

Electronic Properties of Metal Clusters: Size Effects

R. C. BAETZOLD

The effects of size are examined from some properties of model metal clusters by using molecular orbital calculations. Electronic effects were examined for a variety of clusters up to 79 atoms for Au, Ru, Rh, and Pd. In this size range, the binding energy and density of states change drastically with size. We find that p orbitals play a role in the bonding of these clusters, which increases with size. The charge distribution in these clusters results in excess surface electrons as a result of narrower surface bands. Adsorption energies of H$_2$, C$_2$, or O$_2$ molecules on different clusters show a widely varying size dependence, which can be related to electronic properties of the cluster. The addition of ligands to a hypothetical cluster Rh$_6$(CO)$_x$ (x = 2, 6, 12, 16) changes the metal atom DOS to reflect properties of a smaller bare metal cluster.

Introduction

Metal clusters, naked or coordinatively saturated, have been studied from many viewpoints. Experimental approaches to the study of clusters include synthetic,[1] catalytic,[1] chemisorptive,[2] and spectroscopic[3-5] methods. Inherent in many of these studies is the cluster–surface analogy. This analogy deals with the electronic and chemisorptive properties of small metal clusters and their ability to adequately represent metal surfaces. Much of the experimental and theoretical evidence dealing with this question has been discussed.[1,2] A detailed correlation of electronic and chemisorptive properties of small clusters with cluster size would be helpful in probing this analogy.

The synthesis of many cluster compounds[6] of various compositions such as the Rh$_n$(CO)$_m$ (n = 2–14) series makes possible the systematic study of metal properties. Naked metal

clusters have been formed by decarbonylation of these cluster compounds under suitable conditions[7] or by evaporation under vacuum.[8] Hamilton and co-workers have reported catalytic data involving nickel electroless-deposition reactions on naked metal clusters prepared by evaporation,[8] showing effects of cluster size. In each of these studies, the role of ligands in influencing catalytic properties and the extent to which cluster electronic properties represent the analogous surface properties are unknown.

In this paper we examine some electronic properties of clusters as a function of cluster size and as a function of the presence of ligands. In approaching this problem, we use relatively simple molecular orbital calculations such as the extended Hückel theory,[9] which yield valuable insight into the modes of bonding and qualitative trends in behavior of these systems. This method is quite versatile and similar to the tight-binding method useful in solid-state physics. We rely heavily upon experimental information which has been reported for the spectroscopic properties of metal clusters. More

(1) Muetterties, E. L.; Rhodin, T. N.; Band, E; Brucker, C. F.; Pretzer, W. R. *Chem. Rev.* **1979**, 79, 91.
(2) Moskovits, M. *Acc. Chem. Res.* **1979**, 12, 229.
(3) Ozin, G. A.; Huber, H.; McIntosh, D. *Inorg. Chem.* **1977**, 16, 3078.
(4) Unwin, R.; Bradshaw, A. M. *Chem. Phys. Lett.* **1978**, 58, 58.
(5) Mason, M. G.; Gerenser, L. J.; Lee, S.-T. *Phys. Rev. Lett.* **1977**, 39, 288. Mason, M. G.; Hamilton, J. F.; Lee, S.-T.; Nellis, B. F.; Gerenser, L. J.; Logel, P. C., unpublished work.
(6) Longoni, P.; Chini, P. *J. Am. Chem. Soc.* **1976**, 98, 7225.
(7) Smith, G. C.; Chojnacki, T. C.; Dasgupta, S. R.; Iwatate, K.; Watters, K. L. *Inorg. Chem.* **1975**, 14, 1419.
(8) Hamilton, J. F.; Logel, P. C. *Photogr. Sci. Eng.* **1974**, 18, 507; *J. Catal.* **1973**, 29, 253.
(9) Hoffmann, R. *J. Chem. Phys.* **1963**, 39, 1397.